frontiers | Frontiers in Sensors

TYPE Original Research
PUBLISHED 17 July 2025
DOI 10.3389/fsens.2025.1511104

OPEN ACCESS

EDITED BY
Jugal Saharia,
University of Houston–Clear Lake,
United States

REVIEWED BY
Yuqin Shang,
Arizona State University, United States
Andres Vercik,
University of São Paulo, Brazil

*CORRESPONDENCE
Tapan K. Sau,
tapan.sau@iiit.ac.in
Azeemuddin Syed,
syed@psu.edu

RECEIVED 14 October 2024
ACCEPTED 24 June 2025
PUBLISHED 17 July 2025

CITATION
Mazumder A, Biswas A, Sau TK, Bhimalapuram P and Syed A (2025) Radio frequency based detection of specific and nonspecific protein interaction.
Front. Sens. 6:1511104.
doi: 10.3389/fsens.2025.1511104

Radio frequency based detection of specific and nonspecific protein interaction

Annesha Mazumder[1], Arunangshu Biswas[2], Tapan K. Sau[2]*, Prabhakar Bhimalapuram[2] and Azeemuddin Syed[3]*

[1]Center for VLSI and Embedded System Technology, International Institute of Information Technology, Hyderabad, India, [2]Center for Computational Natural Sciences and Bioinformatics, International Institute of Information Technology, Hyderabad, India, [3]School of Engineering, The Behrend College, Pennsylvania State University, Erie, PA, United States

Introduction: Protein detection plays a crucial role in diagnostics and numerous studies. Available protein detection techniques often involve time-consuming and complicated procedures. This report presents a Radio frequency (RF)-based rapid, label-free technique that can be used for differentiation between specific and non-specific binding.

Methods: The utility of the RF-based technique is demonstrated by taking biotin-streptavidin specific interaction as the model system along with other nonspecific proteins. The study involves the use of an interdigitated capacitor-based RF sensor that differentiates the variation in the resonance frequency of the analytes with specific or nonspecific protein binding. The protein binding event is carried out in the presence of gold nanoparticles, which provide the surface for molecular binding and signal amplification.

Results and discussion: The specific binding of biotin-streptavidin is characterized by a constant resonance frequency which does not vary with time or after use of the wash buffer. Contrarily, the resonance frequency shows significant variation in the case of the non-specific interactions like biotin-cytochrome C and biotin-lysozyme. A simulation-based analysis performed using High Frequency Structure Simulator (HFSS) corroborates the finding. The invariant resonance frequency response of the specific protein binding can be utilized as the basis of specific protein detection using RF sensing. The facile RF sensor shows excellent potential as a rapid, reusable, and versatile platform that can be performed remotely without sophisticated laboratory arrangements for protein detection.

KEYWORDS

RF, radio frequency, biosensing, specific-binding, protein

Introduction

Driven by the rapid development in electronics and nanotechnology, biomedical science has witnessed tremendous progress in the last few decades. Steady growth in diagnostics has made it possible to treat diseases that were once considered incurable. An essential aspect of diagnostics deals with antigen identification. A large fraction of antigens are chemically proteins, and as a result, protein identification plays a pivotal role in effectively diagnosing diseases. Most of these antigen detection techniques are based on the characterization of the

specific interaction between antigens and antibodies. The interaction helps to perform both qualitative and quantitative analysis of the antigens involved.

There exist several methods of antigen identification, including the Immunoassay based tests which are very popular in the existing diagnostics market. Immunoassays broadly refer to the techniques where the presence of the target molecule is tested using a receptor molecule having specific affinity for the molecule of interest. Immunoassays can be classified into different types such as Radioimmunoassays (Burrello et al., 2016; Rollag and Niswender, 1976), Fluoroimmunoassays (Zhang et al., 2017; Xu et al., 2017), and Enzyme-linked ImmunoSorbent Assays (ELISA) (Aydin, 2015; Kindt et al., 2007). In any typical immunoassay-based procedure, the receptor molecule, such as an antibody, is attached to the sensor surface and subjected to the analyte consisting of the target molecule. Upon specifically binding to this primary antibody, the system is introduced to the secondary antibody which has been tagged with some label. The label, in turn, could be of various types, such as fluorescent and radioactive. Once the secondary antibody gets attached to the antigen, the interaction between antigens and antibodies can be measured in different ways depending upon the label that is being used. Thus, most of these methods necessitate the use of labels. However, the utilization of labels introduces an additional level of complexity. They involve several stages of incubation and washing, which could even span over a few hours. Additionally, such labels can also damage the biological sample being tested. In short, most of these conventional methods are labor intensive and time consuming. Furthermore, such immunoassay-based processes often require laboratories equipped with sophisticated apparatus/instruments. Such requirements limit their accessibility to a large extent due to the issues related to portability along with the constraints on time and human resources. It poses significant challenges in remote areas where there are severe constraints on resources.

Point of Care (POC) diagnostics and Lab on Chip devices as viable alternatives have caught the attention of the scientific community in recent years. There is a growing interest in developing systems that can remotely identify and quantify antigens without using full-fledged pathological lab facilities. Development of such devices would help in multifarious ways, of which, the most important would be the enhanced accessibility of testing facilities in remote areas. It would also enable rapid testing on a large-scale during times of public health crises. The existence of such well-developed platforms would, in turn, strengthen the public healthcare system, which would indirectly contribute to improving the quality of life for a large section of people. Thus, portable devices that can generate accurate results in a short duration of time, while using the minimum quantities of reagents possible, are currently in high demand.

RF/Microwave-assisted biomedical devices have drawn a considerable amount of interest due to several inherent advantages being conferred by them (Mehrotra et al., 2019; Lee and Yook, 2014). These sensors can be robust, portable and require minute volumes of samples for testing. They offer facile techniques for detection that are associated with reduced complications of sample preparation. In a significant number of cases, these sensors are also label-free, and work based on non-destructive procedures. In many cases, planar RF/microwave devices have become widely popular. They include different RF/microwave structures such as ring resonators (RoyChoudhury et al., 2016; Zarifi and Daneshmand, 2016; Zarifi et al., 2015), interdigitated capacitors (Akhtar et al., 2021; Porwal et al., 2016; Kim, 2008) and waveguides (Tiwari et al., 2017; Wei et al., 2018; Silavwe et al., 2016). These RF/Microwave devices map the changes in different electrical and magnetic quantities such as permittivity and permeability for each material under test (MUT). The variation in these quantities is used as the basis of classification as well as quantification. Furthermore, due to their planar structure, it is easy to integrate such devices with existing technological platforms. RF/Microwave sensors have found many applications across diverse industries. They have been used extensively to perform detection and analysis of different biological and chemical entities. In the medical field, particularly, they have proven to be highly useful. Proteins and various other biomolecules have been detected using various optical, electrical, electromagnetic, etc. sensing techniques including the use of RF sensors to study the pathological and physiological state of cells including cancer cells, dielectric spectroscopy of liquids, various pathogens, biomolecules (Lee and Yook, 2014; Nikolic-Jaric et al., 2009; Grenier et al., 2010; Zhang et al., 2012; Peyman et al., 2015; Surowiec et al., 1988; Wu, 2016; Dalmay et al., 2014; Née Haase et al., 2015; Facer et al., 2001; Mateu et al., 2007; Booth et al., 2010; Song et al., 2006; Ocket et al., 2013; Elsheakh et al., 2013; Narang et al., 2018; Lee et al., 2012; Bahar et al., 2019; Kim et al., 2008; Whitcombe et al., 2011; Akgönüllü et al., 2023; Peinetti et al., 2023; Munoz-Enano et al., 2022; Yang et al., 2010; Mehrotra et al., 2019; Chien et al., 2007) and so on. Although each report has its own merits, there are a number of problems associated with various sensors and there is an immense scope of improvement. Among various problems associated with these sensors, two major issues are: (a) reusability and (b) specificity. The lack of reusability of these sensors arises primarily due to the functionalization of the sensor surface in most cases. The functionalization restricts the use of the sensor for the detection of only certain (class of) fixed analytes. This indirectly necessitates the use of separate kits for the detection of different analytes, which, in turn, complicates the sensor design process. Further, the use of such kits increases the cost of tests. Analyte specificity also poses a challenge since interfering agents could also produce same or similar change in the dielectric constant value of the system. Therefore, it is difficult to assess whether the observed change is due to the analyte of interest or the interfering agents.

In this work, we tried to tackle the above two challenges and present a facile method for rapid detection of specific protein binding using RF sensor. The basic characterization principle involves the mapping of the dependence of the sensor's resonance frequency on the variation of analyte permittivity. The highly specific binding between the target molecule and receptor is always accompanied by a very low dissociation factor and remains relatively unaffected by the change of the surrounding medium in terms of pH, temperature, etc. The Radio frequency-based characterization explores how such specific protein binding differs from nonspecific ones. To prove the concept, we make use of the protein streptavidin binding to biotin, which happens to form the strongest non-covalent bond with a very low dissociation factor. The binding is highly stable and does not vary with changes in the ambient surroundings (Weber et al., 1989; Wong et al., 1999). The specific streptavidin-biotin binding is compared with the responses

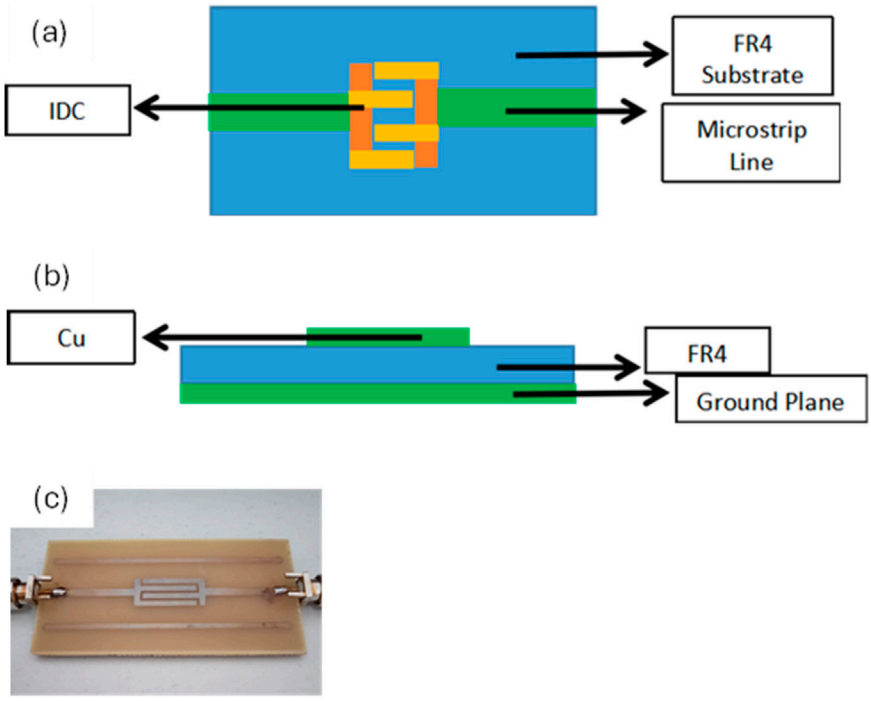

FIGURE 1
IDC sensor: **(a)** Schematic top view, **(b)** Schematic side view, and **(c)** fabricated sensor.

involving nonspecific proteins. The technique does not involve direct functionalization of the sensor surface with any receptor molecule. Instead, the participating analytes are attached to gold nanoparticles which show an inherent affinity for biomolecules. Gold nanoparticles played important roles, viz., provide surface for the binding event and participate in signal generation and amplification. The absence of direct functionalization of the sensor surface not only circumvents the problem of reusability but also ensures that the sensor can be used for conducting the detection of different types of proteins instead of detecting a single protein. The technique is simple, rapid, label-free, efficient, and offers portability. Thus, the RF sensor-based technique appears to be a promising alternative for protein detections.

Results and discussion

Methodology and sensor design

The analysis is performed with the help of an RF interdigitated capacitor (IDC)-based sensor as seen in Figure 1 (Porwal et al., 2016; Kim, 2008). Such sensors consist of comb-like structures which provide high capacitance in a small area and consequently contribute towards improvement in the efficiency of the sensor. They essentially track the variation of the dielectric properties of different materials, which are reflected in the frequency response of the sensors. In our work, the IDC sensor offers a pass-band behavior, with a resonant peak at 5.53 GHz. It consists of two half-wave resonators coupled using an IDC. The interdigitated structure has four fingers, each 12.7 mm long and 1.9 mm wide, with a gap of 0.76 mm between them. The sensor is fabricated on a 1.6 mm thick FR4 substrate with a 0.035 mm copper layer on top and bottom. The maximum electric field is contained in the fingers and the gaps between them. The detailed E-Field analysis has been provided in Supplementary Figures S1-S5 (See Supplementary Material).

In the presence of different materials loaded on top of the sensor, the effective permittivity as seen by the sensor changes, subsequently varying the effective capacitance. This, in turn, is reflected in the frequency response of the sensor. In this work, specifically the emphasis is placed on the resonance frequency, which shifts in the presence of different materials from its unloaded position. Further, the sensor is connected to an Agilent VNA of 6 GHz to measure the frequency response in the form of s-parameters, specifically the reflection coefficient. The signal used in this analysis is the shift in the resonance frequency (Δf) of the sample as compared to the sensor loaded with DI water. Mathematically, this can be given as $\Delta f = f_w - f_s$, where f_w is the resonance frequency of the IDC in presence of DI water and f_s is the resonance frequency of the IDC in presence of the sample under test.

Study of effects of various reagents and analytes on gold nanospheres (GNSPs): UV-Vis spectroscopy

Since the RF sensor responds to the variation in analyte dielectric constants, it is important to understand how the dielectric constants of the systems change when various reagents and analytes are added. The study involves the ligand-receptor kind of interaction for the detection of protein. In order to avoid the non-

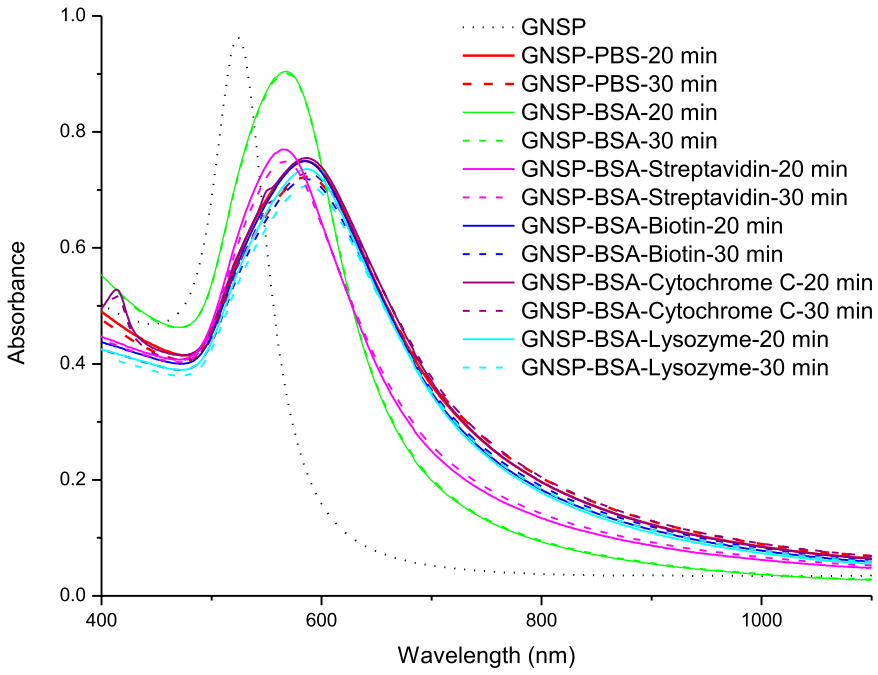

FIGURE 2
Time evolution of Vis-NIR spectra of gold nanospheres (GNSPs) capped with biomolecules of interest in PBS buffer (dotted line for aqueous GNSPs; solid lines for 20 min and dashed lines for 30 min). The reagents/analytes and time of the spectra taken are shown beside the spectra.

specific binding of proteins to gold particle surface, we have used BSA-capped gold nanospheres. PBS buffer maintains a constant pH (pH 6.8) for the system. Addition of large protein molecules to the gold nanoparticle systems results in first particle surface capping and then to some extend particle aggregation. The gold nanoparticles, which were centrifuged after synthesis and redispersed in the same volume DI water, had a hydrodynamic radius of ~35 nm as measured using dynamic light scattering (DLS) and show a wavelength of max. absorbance (λ_m) peak at ~524 nm (Figure 2). Figure 2 and Supplementary Figures S6-S11 (See Supplementary Material) capture the time evolution of various gold nanoparticle systems in PBS buffer. It can be seen that, in the initial 5–10 min window, the λ_m undergoes a red shift and the absorbance decreases. The initial redshift could partly arise from the increase in the dielectric constant surrounding the particles due to the organic protein layer capping of nanoparticles. However, there was negligible change in λ_m and very small change in absorbance (max. 0.0025/min) in the 20–60 min window after reagent additions. We have used the 20–30 min window for the RF measurements. In this 10 minute span, the effects of the surface capping and particle aggregation on the dielectric properties of the system could be neglected.

Study of effects of various reagents and analytes on gold nanospheres (GNSPs): RF resonance frequency shift

The feasibility of performing RF resonance frequency-based analysis of reagents/analytes loaded GNSPs is assessed in this section. The GNSPs residue is dispersed in the 10^{-6} M solutions of various reagents/analytes and allowed to settle for 10 min. It is to be noted that before finalizing the concentrations for the GNSP study using the RF sensor, the samples were individually tested. It was found that beyond the range of 10^{-8} M, the RF sensor does not respond to changes in the Material Under Test (MUT). This in this case, refers to solutions of Biotin, BSA and Streptavidin in PBS Buffer. Thus, considering the biological feasibility as well as the capabilities of the sensor, the final concentration of each for the assessment was taken as 10^{-6} M. Each of these samples are then studied over a period of 10 min. From Figure 3, we observe that RF sensing is capable of studying the changes taking place in the gold nanoparticle systems. In PBS buffer, the resonance frequency shift increases over time. It suggests an increase in the dielectric properties of the system with time. The general trend followed by other sets is that initially the resonance frequency shift decreases for some time and thus, the dielectric constant of the system decreases and then the resonance frequency shift increases. Interestingly, it is important to note that the precise behaviour of the resonance frequency shift for each of these sets is significantly different from one another. This could be due to the difference in the chemical composition, molecular weight of different analytes and their interactions with the gold nanoparticles. The unique signatures generated by these analytes under the test suggest that their binding/aggregation behavior can be effectively studied using RF sensing.

Specific and non-specific binding study: UV-Vis spectroscopy

UV-Vis absorption spectra clearly show the difference between the GNSPs-mediated specific and non-specific bindings of the

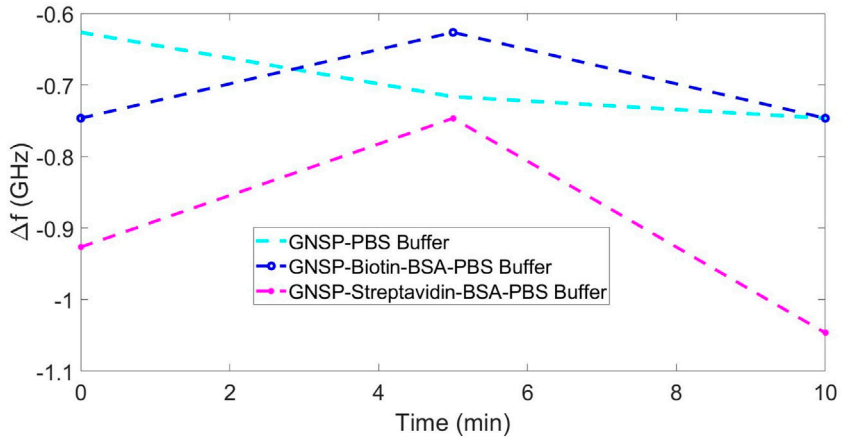

FIGURE 3
Typical RF shift variation behavior of GNSPs in PBS buffer, biotin in PBS buffer and streptavidin in PBS buffer.

proteins. In Figure 4a, we can see that even after the treatment with wash buffer, PBST (Tween-20 dispersed in PBS Buffer), there is no significant shift in the λ_m value for the biotin-streptavidin system. However, in the case of biotin-cytochrome C and biotin-lysozyme, a blue shift can be observed after the treatment with the wash buffer PBST (Figures 4b,c) due to removal of protein layer and hence decrease in dielectric constant. A common observation for both Set A and Set B of each combination, that is biotin-streptavidin, biotin-lysozyme and cytochrome C, is that the absorbance values decrease with the passage of time during the observation period of 10 min. This is valid for samples under test both with and without washing.

Specific and non-specific binding study: resonance frequency shift behaviour

This application demonstrates how protein detection can be performed using the RF sensing technique. Like the other conventional methods for protein detection, the primary detection mechanism in this case also is based on the highly specific antigen-antibody interaction. The sensor's frequency response is analyzed in the presence and absence of the biomolecule to be detected. The idea is that in the case of specific binding, the frequency response would be time-invariant, even if the sample is washed using a wash buffer. However, in the case of non-specific binding, the frequency response would get altered with time. The frequency response would return to the previously occupied blank state if washed with wash buffers. To demonstrate this effect, we have chosen the highly specific biotin-streptavidin interaction. This is the primary ligand-receptor interaction being studied in this case. Further, we have chosen lysozyme and cytochrome C to understand how the frequency response gets altered for non-specific binding. Biotin on the surface of BSA-capped gold nanospheres interacts with streptavidin, cytochrome C or lysozyme. The gold nanospheres help enhance the detection process's efficiency by performing signal amplification. The variation in the interaction of biotin with the specifically bound streptavidin and the non-specifically bound cytochrome C or lysozyme is analyzed. The S_{11} is measured for each sample, and the resonance frequency shift is calculated with respect to the resonance frequency of the sensor in the presence of DI water. The clear difference in the resonance frequency shift behaviour between the specific and non-specific protein bindings can also be seen in the following two ways. First, different proteins, namely, streptavidin, cytochrome C and lysozyme were added to BSA-biotinylated GNSPs, and the resonance frequency shifts were then followed over a period of 10 min. Second, protein-bound BSA-biotinylated GNSPs were treated with wash buffer, PBST. Post washing, the resonance responses were recorded. Figure 5 shows the variation in the resonance frequency shift of these analytes.

From Supplementary Tables SI, SII and SIII (see Supplementary Material), we can note that the response of the three sets being studied varies by a significant margin. As can be observed from Table SI, the resonance frequency shift of biotin-streptavidin becomes stable after roughly 5 min. This period could be indicative of the time the complex requires to bind completely. The resonance frequency shift is low initially and after 5 min, it settles at −0.9266 GHz, indicating that the effective capacitance increases as the complex moves towards a stable configuration. This is expected since once the complex reaches maximum stability, the measured physical and chemical parameters remain unchanged due to the irreversible nature of the bond.

The second half of the experiment was crucial for confirming the correct detection of specific binding by the RF sensor. Wash Buffers are extensively used in immunoassay-based processes where they are used to eliminate weakly interacting or unbound analytes. The basic principle behind it is that specific binding alone survives the interaction with wash buffers, whereas non-specific binding gets removed. In the case of biotin-streptavidin, since they bind specifically, the bonds will remain intact even after washing. As a result of this, even the frequency response of the system shall remain the same when compared against the frequency response of the system before the application of the wash buffer. As depicted in Figure 5, the resonance frequency shift remains unchanged after washing biotin-streptavidin. This stability observed in the case of biotin-streptavidin is in stark contrast with the case of biotin-lysozyme and biotin-cytochrome C wherein the resonance frequency shift varies dramatically after being washed by PBST.

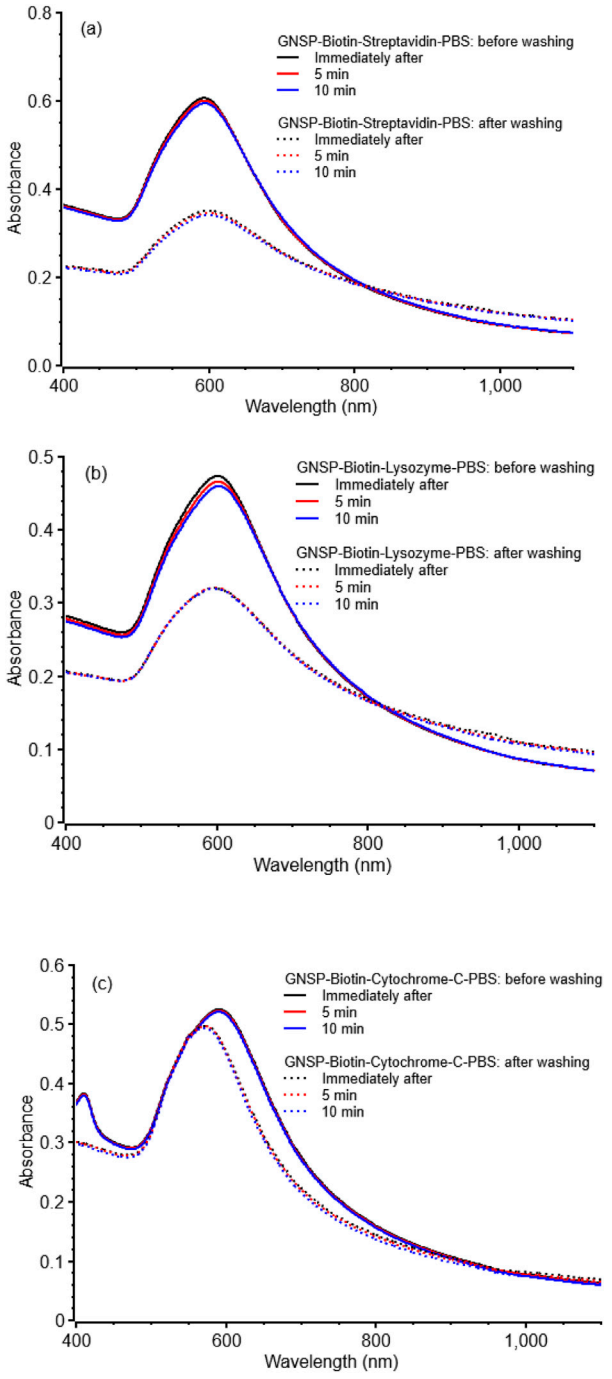

FIGURE 4
UV-Vis spectra for specific [**(a)** biotin-streptavidin] and non-specific [**(b)** biotin-lysozyme, **(c)** biotin-cytochrome-C] binding, before and after the treatment with wash buffer.

In particular, we can observe that the resonance frequency shift value at the end of the observation period of Set A and Set B remains unchanged for biotin-streptavidin. In fact, the resonance frequency shift remains constant at −0.9266 GHz throughout the observation period of Set B. The same, however, is not true for biotin-cytochrome C and biotin-lysozyme. In both cases, the resonance frequency shift observed during the observation period of Set B was significantly different from that observed for Set A for each of them. In the case of specific binding, it resembles an antigen-antibody kind of interaction that is capable of tolerating washing. However, in case of non-specific binding, the binding is weak and gets easily broken by the wash buffer. It is interesting to note that the behaviour exhibited by these two complexes is different from each other. In the case of lysozyme, the resonance frequency shift measured at the end of the observation period of Set B varies from that observed at the end of Set A by nearly 32%. The resonance frequency shift of −0.6266 GHz is recorded throughout the measurement timeframe of Set B with no variation. This behaviour is different from cytochrome C wherein the resonance frequency shift during the measurement period of Set B varies between −1.13 GHz and −1.04 GHz. The final value at the end of Set B varies from the final value at the end of set A measurement for cytochrome C, by about 3%. Thus, the amount by which the resonance frequency shift varies in Set A and Set B is different in the case of lysozyme and cytochrome C. One possible reason behind this could be the variation in the molecular weight (MW) of the two analytes. While lysozyme has a MW of 14,000 Da, cytochrome C has a MW of 12,000 Da. It can be expected that the variation in resonance frequency shift between Set A and Set B is related to the MW of the analyte which binding to biotin. Another plausible explanation for this observation could be that the binding in case of biotin-cytochrome C is comparatively stronger than that in biotin-lysozyme. The variation in resonance frequency shift is much higher in case of lysozyme as compared to that of cytochrome C. Additionally, in case of biotin-lysozyme, after getting washed with PBST, the resonance frequency shift decreases indicating that the resonance frequency of the sample resembles distilled water more closely as compared to the samples of the other complexes. This, in turn, implies that washing with PBST has reduced the concentration of the biotin-lysozyme complex due to its weak interaction. This decrease in concentration is lesser as compared to that of biotin-cytochrome C. The resonance frequency curves at the end of the measurement periods of Set A and Set B have also been given in Supplementary Figures S12-S14 (See Supplementary Material). The figures help to further illustrate the variation in the response between specific and non-specific binding. Thus, these results indicate that if the interaction between the receptor, biotin and the analyte under test (streptavidin, lysozyme or cytochrome C) changes, the resonance frequency changes due to underlying variation in the capacitance of the sensor and the effective permittivity.

Simulation based study of resonance frequency shift behaviour of specific and non-specific binding

To further strengthen the idea that with variation in interaction the resonance frequency changes, we performed a set of simulations in HFSS, which imitates the process of specific and non-specific binding. It is important to clarify that the sizes of the particles utilized in this case were representative in nature, and in absolute terms, were much larger than the sizes utilized in the experimental study. This was a preliminary study to establish that using such computational analyses the exploration of analyte-receptor binding can be characterized using RF. Specifically, the intention was to show

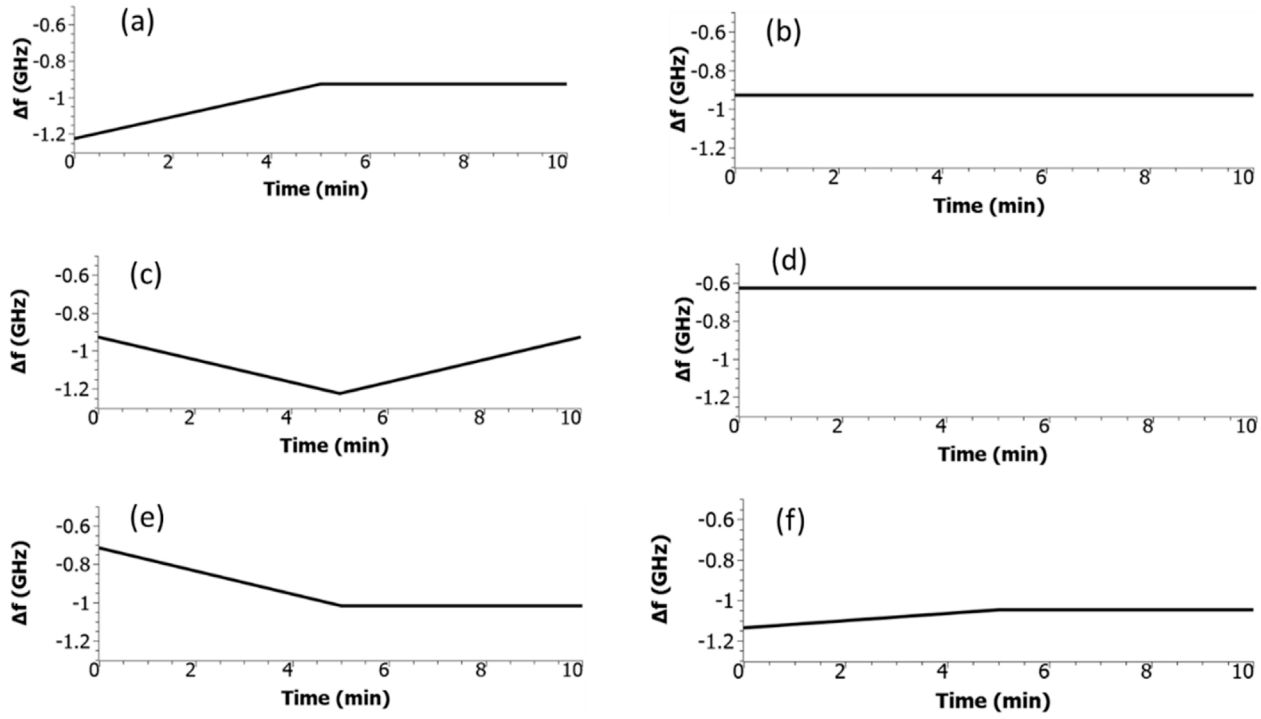

FIGURE 5
Variation of resonance frequency shift of: (Left panel) protein binding to BSA-biotinylated GNSPs and (Right panel) protein bound BSA-biotinylated GNSPs after treatment with wash buffer. **(a,b)** biotin-streptavidin, **(c,d)** biotin-lysozyme and **(e,f)** biotin-cytochrome C systems.

that the relative arrangement of particles, can impact the frequency response of the sensor. This was to further the primary hypothesis of this work which argues that the difference in the RF sensor's response occurs due to both the interaction between the particles and the changes in their relative arrangement. In other works, both of these contribute to the effective changes in the dielectric behavior and the section below has attempted to capture it.

An IDC based RF sensor resonating at 66.76 GHz was taken for the analysis. The IDC cavity comprises four fingers of 1.06 mm length and 0.16 mm width, with a spacing of 0.063 mm between the fingers. An insulating layer was placed on top of the IDC cavity and the sample in aqueous form was introduced due to this insulating layer. An aqueous solution of thirty gold particles of radius 300 nm was taken and each of these particles were coated with a layer receptor molecules of thickness 400 nm. To demonstrate the occurrence of specific binding, these protein-conjugated gold particles were further coated with a layer of specifically binding analyte of 900 nm thickness. On the other hand, to exhibit the presence of non-specific binding, the particles of the non-specifically binding analyte were roughly dispersed around the protein-conjugated gold particles. Three such arrangements (Refer to Supplementary Figures S15-S18) were studied. Different arrangements were assessed for the non-specific binding, while for the specific binding a uniform layer was used. This was done to mimic the stability of the specific binding and the relative instability or dynamic nature of the non-specific binding instances.

For specific binding we observe a frequency shift of −0.64 GHz while for the non-specific binding, the resonance frequency shifts for the three cases are −0.11 GHz, −0.19 GHz and −0.08 GHz. The results indicate that when the arrangement of the non-specifically binding analyte is varied, the resonance frequency shift varies. Furthermore, each of these shifts are different from the resonance frequency measured for the specific binding case. Thus, even for the same volume of total sample used, the response varies. This indicates that in addition with the concentration or volume of the MUT, the arrangement, morphology and interaction between particles impact the dielectric behavior. Thus, this in turn validates the idea that with variation in the binding of the analytes, the frequency response of the sensor will change and subsequently, alter the calculated resonance frequency shift.

Conclusion

An IDC RF sensor is fabricated and employed for the characterisation of the specific and non-specific binding of proteins which can be the basis of protein detection. BSA-capped biotinylated gold nanoparticles were used to demonstrate protein detection. Three proteins, namely streptavidin, cytochrome C and lysozyme were used. The influence of the various analytes/reagents on the time evolution of the systems has been assessed both UV-Vis spectroscopic and RF sensor measurements. The biotin-streptavidin system, which is characterised by a specific binding, is found to have a time-invariant resonance frequency shift. The response remains unaltered even after the solution has been washed with PBST wash buffer, which further confirms the formation of specific binding. In the case of non-specific binding, the resonance frequency shift keeps

changing, indicating weak non-specific interactions between biotin and lysozyme or cytochrome C. The frequency response varies by a wide margin after being introduced to the wash buffer, PBST, contrary to the case of specific binding. Simulation-based study of the resonance frequency shift behaviour of specific and non-specific binding of model systems support the experimental observations. The resonance frequency shift vs. analyte concentration plot shows a linear relationship. This suggests that RF sensors can be used for efficient and rapid detection of proteins.

Methods

Sensor design

The analysis is performed using an IDC based RF sensor, resonating at 5.53 GHz. The IDC section is used to couple two half-wave resonators. The interdigitated structure has four fingers which are each 12.7 mm long and 1.9 mm wide with a gap of 0.76 mm between them. The sensor is fabricated on a 1.6 mm thick FR4 substrate with a 0.035 mm copper layer on top.

Experimental setup

The experimental setup comprises a Vector Network Analyzer (VNA) from Agilent Technologies, connected to the Device Under Test (DUT) using SMA cables of 50 Ω (See Supplementary Figure S19). The VNA (N9923A) works from 2 MHz to 6 GHz. The VNA is calibrated using the standard SOLT technique with an IF bandwidth of 10 kHz. The DUT, in this case, is an interdigitated capacitor-based RF Sensor. The VNA is used to characterize the MUT by observing the changes occurring in the s-parameters.

Analytes under study

Biotin is the receptor used for capturing the analyte of interest. It is a water-soluble vitamin that is present in all living organisms in small quantities. Streptavidin is the primary analyte which is detected with the help of its conjugate receptor, biotin. It is a tetrameric biotin-binding protein that is isolated from *Streptomyces* avidinii. It forms the strongest non-covalent bond with biotin with a dissociation factor as low as 10^{-15}. The interaction is highly specific and is widely exploited for conducting immunoassays. Lysozyme is the secondary analyte and its non-specific interaction with the receptor molecule, biotin is studied. Like lysozyme, cytochrome C is also a secondary analyte and is used for studying non-specific interactions. It is a water-soluble mitochondrial intermembrane space protein that is loosely attached to the inner mitochondrial membrane. Bovine Serum Albumin or BSA is a globular protein that is frequently used in biochemical applications as a blocking agent. In this study, it binds to the gold nanoparticle surface and the receptor, biotin, and restricts the non-specific interactions of gold nanoparticle with other analytes.

Reagents and materials

Biotin, streptavidin, cytochrome C, lysozyme and BSA were obtained from SRL Chemicals. Sodium borohydride and ascorbic acid used for the gold nanosphere synthesis were obtained from Sigma Aldrich while cetyltrimethylammonium bromide (CTAB) obtained from SRL Chemicals. Sodium phosphate dibasic and the monopotassium phosphate used for pH adjustment were bought from Finar Chemicals and SRL Chemicals, respectively. Tween-20 used for Wash Buffer preparation was obtained from SRL Chemicals.

Preparation of gold nanospheres (GNSPs)

The GNSP solution is prepared following the seed-mediated technique reported earlier (Sau and Murphy, 2004). The methodology involves two major steps- (i) the synthesis of small seed particles and (ii) the development of the required gold nanospheres using the seed prepared in (i).

Preparation of seed solution

In order to prepare the seed solution, CTAB solution and $NaBH_4$ solution, are first prepared. 0.1 M CTAB solution is prepared by dissolving the required amount of CTAB in Millipore water and mixing it using a magnetic stirrer. The CTAB solution should not be more than 30 days old for the GNSP synthesis. 0.01 M of $NaBH_4$ solution is prepared next by adding $NaBH_4$ to ice-cooled Millipore water. $NaBH_4$ solution were freshly prepared to ensure the correct formation of seed. The seed solution is prepared using ice-cold sodium borohydride ($NaBH_4$) solution as the reducing agent, $HAuCl_4$ solution as the gold precursor and CTAB as the capping agent. 3 mL of 0.1 M CTAB is first added to Millipore water and then 100 μL of the gold precursor, $HAuCl_4$ solution, is added to the mixture. The solution is a bright golden yellow at this stage. After this, 240 μL the ice-cold $NaBH_4$ solution is added carefully, and the colour of the solution changes to brown. After the addition of each reagent, the solution is first mixed with the help of inversion mixing and then using a Vortex mixer. This is essential to ensure that the mixing has taken place uniformly. The seed solution is allowed to settle for at least 2 h before being used for making the gold spheres.

Preparation of GNSP from seed solution

The GNSP growth solution is prepared using Ascorbic Acid (AA) as a reducing agent, CTAB as the capping agent and $HAuCl_4$ as the precursor. 5 mL of 0.1 M AA solution is freshly prepared by adding the required amount of AA to Millipore water. To prepare 10 mL of gold nanospheres, 160 μL of 0.1 CTAB solution is added to 9.0352 mL of Millipore water and mixed. 200 µL of $HAuCl_4$ is added next which turns the solution golden yellow. Upon adding 600 μL of AA, the solution turns colourless due to the reduction of Au^{3+} ions. 4.8 μL of seed solution is carefully added at the end. After mixing the solution using the vortex mixer, it starts turning pink. It attains a bright wine red colour after some time. It was kept at rest for at least 6 h before being taken for centrifugation. The GNSP are centrifuged at 10,000 r.p.m. for 15 min.

Preparation of wash buffer

50 mL of the Wash Buffer is prepared by adding 5 mL of PBS Buffer of pH 6.8 and 0.05 mL of Tween-20 in Millipore water.

Preparation of samples for resonance frequency shift study of specific and non-specific binding

Gold nanospheres were prepared using CTAB as capping agent as described in Methods section. These gold nanoparticles were centrifuged, and the residue was preserved for further preparation of reagents. 10^{-4} M solutions of biotin, streptavidin, cytochrome C, lysozyme and BSA were prepared in PBS buffer solution of pH 6.8. The gold nanosphere residue was dispersed in 10^{-6} M solution of biotin in BSA-PBS solution and allowed to settle for 5 minutes. This gold conjugated solution of Biotin-BSA was then taken for centrifugation. The sample for centrifuged at 8,000 r.p.m. for 1 min. The residue from the biotin-BSA-gold nanosphere conjugate was dispersed in solutions of 10^{-6} solutions of streptavidin, lysozyme and cytochrome C separately. Two such sets A and B were prepared for each complex, that is, biotin-streptavidin, biotin-cytochrome C and biotin-lysozyme. All the samples of Set A were allowed to settle for 15 min before being taken for testing, while those of Set B were allowed to settle for 25 min. Set B of each combination was centrifuged at 6,000 r.p.m. for 3 min after being allowed to settle for 25 min and any unbound analyte was removed with the supernatant. The residue from the centrifugation step was dispersed in solutions of Wash Buffer. The Wash Buffer was prepared by mixing Tween-20, a non-ionic surfactant with the PBS Buffer solution in appropriate proportion. Set B was treated with the Wash Buffer for 20 min. Like Set A, Set B of each combination was also tested on the Radiofrequency sensor for 10 min each.

Data availability statement

The raw data supporting the conclusions of this article will be made available by the authors, without undue reservation.

Author contributions

AM: Validation, Writing – review and editing, Data curation, Formal Analysis, Investigation, Methodology, Writing – original draft. AB: Methodology, Writing – review and editing. TS: Writing – review and editing, Conceptualization, Formal Analysis, Funding acquisition, Investigation, Project administration, Resources, Supervision, Validation. PB: Conceptualization, Formal Analysis, Funding acquisition, Investigation, Project administration, Resources, Supervision, Validation, Writing – review and editing, Data curation, Methodology. AS: Conceptualization, Funding acquisition, Project administration, Resources, Supervision, Validation, Writing – review and editing.

Funding

The author(s) declare that financial support was received for the research and/or publication of this article. This work was supported by the Department of Biotechnology (DBT), Govt. of India, as a part of the project “Design of Radio Frequency Cavities for Detection of Specific Protein” (DBT Ref no. BT/PR20720/MED/32/590/2017).

Acknowledgments

AM thanks IHub-Data, IIIT Hyderabad, for a research fellowship.

Conflict of interest

The authors declare that the research was conducted in the absence of any commercial or financial relationships that could be construed as a potential conflict of interest.

Generative AI statement

The author(s) declare that no Generative AI was used in the creation of this manuscript.

Publisher’s note

Supplementary material

The Supplementary Material for this article can be found online at: https://www.frontiersin.org/articles/10.3389/fsens.2025.1511104/full#supplementary-material

References

Akgönüllü, S., Kılıç, S., Esen, C., and Denizli, A. (2023). Molecularly imprinted polymer-based sensors for protein detection. *Polymers* 15, 629. doi:10.3390/polym15030629

Akhtar, M. J., Tiwari, N. K., and Govind, G. (2021). Idc planar rf sensors for dielectric testing and applications. *Interdigital Sensors* 199, 199–229. doi:10.1007/978-3-030-62684-6_8

Aydin, S. (2015). A short history, principles, and types of elisa, and our laboratory experience with peptide/protein analyses using elisa. *Peptides* 72, 4–15. doi:10.1016/j.peptides.2015.04.012

Bahar, A., Zakaria, Z., Arshad, M., Isa, A., Dasril, Y., and Alahnomi, R. (2019). Real time microwave biochemical sensor based on circular SIW approach for aqueous dielectric detection. *Sci. Rep.* 9, 1–12. doi:10.1038/s41598-019-41702-3

Booth, N., Orloff, J.C. ad, Mateu, J., Janezic, M., Rinehart, M., and Beall, J. (2010). Quantitative permittivity measurements of nanoliter liquid volumes in microfluidic channels to 40 ghz. *IEEE Trans. Instrum. Meas.* 59, 3279–3288. doi:10.1109/tim.2010.2047141

Burrello, J., Monticone, S., Buffolo, F., Lucchiari, M., Tetti, M., Rabbia, F., et al. (2016). Diagnostic accuracy of aldosterone and renin measurement by chemiluminescent immunoassay and radioimmunoassay in primary aldosteronism. *J. Hypertens.* 34, 920–927. doi:10.1097/hjh.0000000000000880

Chien, J. H., Chen, P. H., Kuo, L. S., Lin, C. S., and Wang, H. (2007). Protein detection using a radio frequency biosensor with amplified gold nanoparticles. *Appl. Phys. Lett.* 91, 143901. doi:10.1063/1.2794758

Dalmay, C., Leroy, J., Pothier, A., and Blondy, P. (2014). Development of high frequency microfluidic biosensors for intracellular analysis. *Procedia Eng.* 87, 54–57. doi:10.1016/j.proeng.2014.11.264

Elsheakh, D., Elsadek, H., Abdullah, E., Atteya, S., and Elmazny, W. (2013). "Novel rapid detection of different viruses in blood using microimmuno-sensor," in *2013 7th European conference on antennas and propagation (EuCAP)* (IEEE), 1128–1131.

Facer, G., Notterman, D., and Sohn, L. (2001). Dielectric spectroscopy for bioanalysis: from 40 hz to 26.5 ghz in a microfabricated wave guide. *Appl. Phys. Lett.* 78, 996–998. doi:10.1063/1.1347020

Grenier, K., Dubuc, D., Poleni, P., Kumemura, M., Toshiyoshi, H., and Fujii, T. (2010). "Resonant based microwave biosensor for biological cells discrimination," in *2010 IEEE Radio and wireless symposium (RWS)* (IEEE), 523–526.

Kim, J. Development of interdigitated capacitor sensors for direct and wireless measurements of the dielectric properties of liquids. (2008).

Kim, J., Babajanyan, A., Hovsepyan, A., Lee, K., and Friedman, B. (2008). Microwave dielectric resonator biosensor for aqueous glucose solution. *Rev. Sci. Instrum.* 79, 086107. doi:10.1063/1.2968115

Kindt, T., Goldsby, R., Osborne, B., and Kuby, J. (2007). *Kuby immunology*. Macmillan.

Lee, H., Lee, J. H., Moon, H. S., Jang, I. S., Choi, J. S., Yook, J. G., et al. (2012). A planar split-ring resonator-based microwave biosensor for label-free detection of biomolecules. *Sensors Actuators B Chem.* 169, 26–31. doi:10.1016/j.snb.2012.01.044

Lee, H., and Yook, J. (2014). Recent research trends of radio-frequency biosensors for biomolecular detection. *Biosens. Bioelectron.* 61, 448–459. doi:10.1016/j.bios.2014.05.025

Mateu, J., Orloff, N., Rinehart, M., and Booth, J. (2007). "Broadband permittivity of liquids extracted from transmission line measurements of microfluidic channels," in *2007 IEEE/MTT-S international microwave symposium* (IEEE), 523–526.

Mehrotra, P., Chatterjee, B., and Sen, S. (2019). EM-wave biosensors: a review of RF, microwave, mm-wave and optical sensing. *Sensors* 19, 1013. doi:10.3390/s19051013

Munoz-Enano, J., Peytral-Rieu, O., Velez, P., Dubuc, D., Grenier, K., and Martin, F. (2022). Characterization of the denaturation of bovine serum Albumin (BSA) protein by means of a differential-mode microwave microfluidic sensor based on slot resonators. *IEEE Sensors J.* 22, 14075–14083. doi:10.1109/jsen.2022.3181542

Narang, R., Mohammadi, S., Ashani, M. M., Sadabadi, H., Hejazi, H., Zarifi, M. H., et al. (2018). Sensitive, real-time and non-intrusive detection of concentration and growth of pathogenic bacteria using microfluidic-microwave ring resonator biosensor. *Sci. Rep.* 8, 15807–15810. doi:10.1038/s41598-018-34001-w

Née Haase, N., Fuge, T. G. H. K., Zeng, A., and Jacob, A. (2015). Miniaturized transmission-line sensor for broadband dielectric characterization of biological liquids and cell suspensions. *IEEE Trans. Microw. Theory Tech.* 63, 3026–3033. doi:10.1109/tmtt.2015.2472009

Nikolic-Jaric, M., Romanuik, S. F., Ferrier, G. A., Bridges, G. E., Butler, M., Sunley, K., et al. (2009). Microwave frequency sensor for detection of biological cells in microfluidic channels. *Biomicroflu- idics* 3, 034103. doi:10.1063/1.3187149

Ocket, I., Song, L., Grillet, D., and Embrechts, B. (2013). "Dielectric characterization of biological liquids and tissues up to 110 ghz using an ltcc cpw sensor," in *2013 IEEE topical conference on biomedical wireless Technologies, networks, and sensing systems* (IEEE), 43–45.

Peinetti, F., Yasir, M., and Savi, P. (2023). RF sensor with graphene film for HRP concentration detection. *C* 9, 63. doi:10.3390/c9030063

Peyman, A., Kos, B., Djokić, M., Trotovšek, B., Limbaeck-Stokin, C., Serša, G., et al. (2015). Variation in dielectric properties due to pathological changes in human liver. *Bioelectromagnetics* 36, 603–612. doi:10.1002/bem.21939

Porwal, P., Syed, A., Bhimalapuram, P., and Sau, T. (2016). "Detection of biotin-streptavidin interaction using rf interdigitated capacitive cavity," in *2016 IEEE MTT-S international microwave and RF conference (IMaRC)* (IEEE), 1–4.

Rollag, M., and Niswender, G. (1976). Radioimmunoassay of serum concentrations of melatonin in sheep exposed to different lighting regimens. *Endocrinology* 98, 482–489. doi:10.1210/endo-98-2-482

RoyChoudhury, S., Rawat, V., Jalal, A., Kale, S., and Bhansali, S. (2016). Recent advances in metamaterial split-ring-resonator circuits as biosensors and therapeutic agents. *Biosens. Bioelectron.* 86, 595–608. doi:10.1016/j.bios.2016.07.020

Sau, T. K., and Murphy, C. J. (2004). Seeded high yield synthesis of short Au nanorods in aqueous solution. *Langmuir* 20, 6414–6420. doi:10.1021/la049463z

Silavwe, E., Somjit, N., and Robertson, I. D. (2016). A microfluidic-integrated siw lab-on-substrate sensor for microliter liquid characterization. *IEEE Sensors J.* 16, 7628–7635. doi:10.1109/jsen.2016.2599099

Song, C., Syed, A., Lee, B., Harackiewicz, F., Yen, M., Ralu, D., et al. (2006). "Microwave dielectric properties of on-chip liquid films," in *2006 IEEE/NLM life science systems and applications workshop* (IEEE), 1–2.

Surowiec, A., Stuchly, S., Barr, J., and Swarup, A. (1988). Dielectric properties of breast carcinoma and the surrounding tissues. *IEEE Trans. Biomed. Eng.* 35, 257–263. doi:10.1109/10.1374

Tiwari, N. K., Singh, S. P., and Akhtar, M. J. (2017). "Coplanar waveguide based planar rf sensor for the detection of adulteration in oils," in *2017 IEEE applied electromagnetics conference (AEMC)*, 1–2.

Weber, P., Ohlendorf, D., Wendoloski, J., and Salemme, F. (1989). Structural origins of high-affinity biotin binding to streptavidin. *Science* 243, 85–88. doi:10.1126/science.2911722

Wei, Z., Huang, J., Li, J., Xu, G., Ju, Z., Liu, X., et al. (2018). A high-sensitivity microfluidic sensor based on a substrate integrated waveguide *re*-entrant cavity for complex permittivity measurement of liquids. *Sensors* 18, 4005. doi:10.3390/s18114005

Whitcombe, M. J., Chianella, I., Larcombe, L., Piletsky, S. A., Noble, J., Porter, R., et al. (2011). The rational development of molecularly imprinted polymer-based sensors for protein detection. *Chem. Soc. Rev.* 40, 1547–1571. doi:10.1039/c0cs00049c

Wong, J., Chilkoti, A., and Moy, V. (1999). Direct force measurements of the streptavidin–biotin interaction. *Biomol. Eng.* 16, 45–55. doi:10.1016/s1050-3862(99)00035-2

Wu, H. (2016). Label-free and antibody-free wideband microwave biosensor for identifying the cancer cells. *IEEE Trans. Microw. Theory And Tech.* 64, 982–990. doi:10.1109/TMTT.2016.2515098

Xu, J., Haupt, K., and Tse Sum Bui, B. (2017). Core–shell molecularly imprinted polymer nanoparticles as synthetic antibodies in a sandwich fluoroimmunoassay for trypsin determination in human serum. *ACS Appl. Mater. and interfaces* 9, 24476–24483. doi:10.1021/acsami.7b05844

Yang, Y., Zhang, H., Zhu, J., Wang, G., Tzeng, T. R., Xuan, X., et al. (2010). Distinguishing the viability of a single yeast cell with an ultra-sensitive radio frequency sensor. *Lab. Chip* 10, 553–555. doi:10.1039/b921502f

Zarifi, M., Thundat, T., and Daneshmand, M. (2015). High resolution microwave microstrip resonator for sensing applications. *Sensors Actuators A Phys.* 233, 224–230. doi:10.1016/j.sna.2015.06.031

Zarifi, M. H., and Daneshmand, M. (2016). Wide dynamic range microwave planar coupled ring resonator for sensing applications. *Appl. Phys. Lett.* 108, 232906. doi:10.1063/1.4953465

Zhang, H., Xu, T., Gao, L., Liu, X., Liu, J., and Yu, B. (2017). A novel fluoroimmunoassay for detecting ruscogenin with monoclonal antibodies conjugated with cdse/zns quantum dots. *Molecules* 22, 1250. doi:10.3390/molecules22081250

Zhang, L., Morand du Puch, C., Lacroix, A., Dalmay, C., Pothier, A., and Lautrette, C. (2012). "Microwave biosensors for identifying cancer cell aggressiveness grade," in *2012 IEEE/MTT-S international microwave symposium digest* (IEEE), 1–3.